International Journal of Engineering & Technology, 7 (3.31) (2017) 86-92

International Journal of Engineering & Technology

Website: www.sciencepubco.com/index.php/IJET

Research paper

Multi-Scale Principal Component Analysis for the Fault Detection and Isolation in Induction Motors

Naga Venkata Navya Repaka, Vidya Sagar Yellapu*

Department of Electrical and Electronics Engineering, SRKR Engineering College, Bhimavaram, Andhra Pradesh, India- 534204
**Corresponding AuthorE-mail: navyasri.repaka@gmail.com ; Tel:+91- 8096601611*

Abstract

Induction motors, though rugged, undergo faults due to wear and tear in their operation. Some faults have the characteristic property of influencing the stator current frequencies. Some side-band frequencies can be observed in the case of such faults. In this paper, a Multi-Scale Principal Component Analysis which combines wavelet analysis with principal component analysis has been applied to the data obtained from the simulation model of an induction motor. A 3-level decomposition of the data is performed and the principal component analysis is applied to high-frequency and low-frequency components of the data at various levels. The results suggest the use of the scheme for timely detection and identification of the faults which would endanger the motor from the otherwise possible destruction. It has also been proved that the scheme has the capability of detecting the sensor faults also, in addition to the motor faults.

Keywords: *Induction motor; multi-scale principal component analysis; side-band frequencies; wavelet analysis.*

1. Introduction

Induction motors are widely used in many industrial applications because of their low cost. During their operation, the induction motors can undergo faults due to incorrect operating conditions, manufacturing defects, harsh environment etc. There is high potential for the destruction of motor, if the faults are not detected in time. The types of faults present in induction motor are electrical faults: classified as stator and rotor faults; and mechanical faults: classified as air gap eccentricity and bearing faults [1]. Out of all these faults, some faults develop frequency dependent features, which when analyzed, lead to their detection and identification of the cause. Such faults are broken rotor bar, air-gap eccentricity, bearing damage, loading effects, shorted turn in stator windings [2].

Techniques such as Fast Fourier Transform are useful for the frequency estimation of features but their use is limited to stationary signals and the information regarding time of occurrence of fault is missing. Hence, techniques such as Short Time Fourier transform (STFT) and Wavelet Transform (WT) are into picture to account also for the time information. In STFT, the analysis window size is fixed but in WT, the use of analyzing functions, called wavelets, adjust their time-widths to their frequency in such a way that high frequency wavelets will be very narrow and low frequency ones are broader. WT has the ability to identify the changes in the frequency at some its time-scales. WT has become a very popular technique for FDI [3, 4].

When the high-frequency components (details) are removed from the data, the resulting low frequency components (approximations) are taken to represent the noise-free true variations of the signals. The relationships among the approximations of the signals can be found through techniques such as Principal Component Analysis (PCA)[5] to deduce features to detect the faults. However, a most sophisticated technique such as Multi-Scale Principal Component Analysis (MSPCA)[6] can be used to combine wavelet analysis, which decomposes a signal in to difference time-scale resolution, with the, which extracts relationships among the signals used in the wavelet analysis.

In this paper, the use of MSPCA for the Fault Detection and Isolation (FDI) of faults with different frequency features in induction motors is tested. The required data of stator currents is generated through a simulation model of a 3-phase induction motor. This model develops a balanced set of stator currents which would flow in one of the typical operating conditions. Some suitable noise is superimposed onto these signals to get the realistic operating conditions. The side-band frequencies corresponding to some probable fault modes of the induction motor are also added in the signals to simulate faulty behavior. The resulting signals are given to the MSPCA based algorithm for FDI and the effectiveness is established.

The rest of the paper is organized as follows: Section 2 describes different fault modes that take place in an induction motor and that exhibit different side-band frequencies in the stator currents. Section 3 describes the PCA model development. Section 4 details the WT and MSPCA. Section 6 presents the simulation model of the induction motor. Results are described in Section 7. Finally, conclusions are drawn in Section 8.

.

1. 2. Various Faults in Induction Motors That Lead To Variations in the Frequency Spectrum

In this section, various faults in induction motors that lead to variations in the frequency spectrum are described in brief. For each fault, the side-band frequencies and their description is given in **Table 1.**

2.1. Broken Rotor Bars

The main cause for broken rotor bars are pulsating mechanical loads, direct online starting. [7] The BRB fault in the motor can cause the overheating and sparking.

2.2. Air-gap Eccentricity

Table 1:. Side-band frequencies for different faults.

S.No.	Fault Type	Side-band frequencies	Equation terms
1.	Broken rotor bars	$f_{brb} = * f_g\left[K\left(\frac{1-S}{P}\right) \pm S\right]$	$f_{brb}$is broken rotor bar frequency k = 1, 2, 3, ….
2.	Air-gap eccentricity	$f_{ec} = f_g\left[(R \pm n_d)\left(\frac{(1-S)}{P}\right) \pm n_{ws}\right]$	$f_{ec}$is eccentricity frequency. R is the number of rotor bars. n_d= ±1 n_{ws}= 1, 3, 5, 7 …
3.	Bearings damage.	$f_0 = 0.4nf_{rm}$ $f_1 = 0.6nf_{rm}$	$f_0$is lower side-band frequency, $f_1$is upper side-band frequency, n is the number of balls in the bearings. $f_{rm}$is the rotor's mechanical frequency.
4.	Shorted-turns in stator windings.	$f_{load} = f_g\left[1 \pm m\left(\frac{(1-s)}{p}\right)\right]$	$f_{st}$is the component related to shorted turn. n = 1,2,3,…

*f_g is electrical supply (grid) frequency;** p is number of pole pairs. s is per unit slip.

The non-magnetic part of a magnetic circuit in machines is called Air gap. The air gap is connected magnetically in series with the remaining of the circuit, so that a substantial part of the magnetic flux flows through the gap. Air gap is left in induction motors for the flow.

In between stator and the rotor has magnetic flux. The air gap is generally uniform in all the radial directions from the rotor. However, some situations may arise into unequal air gaps known as eccentricity. This eccentricity is dividing into two types Static eccentricity and dynamic eccentricity [7]. In case of static eccentricity, the position of the minimal radial air gap length is fixed in space. Incorrect positioning of the stator or rotor core at the commissioning stage results into static eccentricity. While for the dynamic, the centre of the rotor and the rotational centre do not coincide; so that the minimum air gap rotates unacceptable levels of them will occur after the motor has been running for a number of years. This misalignment causes several factors such as bent rotor shaft, bearing wear etc.

2.3. Bearings Damage

Bearings are generally damaged at inner and outer races due to continuous stress on them. Contamination, corrosion, improper lubrication, unbalanced shaft voltages, flux disturbance like rotor eccentricities, temperatures are also the main reasons to cause the bearing failures. These kinds of failures results in the detectable vibrations and increased noise levels [8].

2.4. Shorted turn in Stator Windings

Inter turn faults in stator windings usually occur due to breakdown of insulation [7]. These faults are phase-to-phase or phase-to-ground faults. The destruction of motor may occur if these faults are not detected in time. The various causes for stator faults are Thermal stress and Mechanical stress [2].

3. Principal component Analysis (PCA)

PCA is a multi-variate statistical technique mostly used in FDI, which works based on the relations between the variables in terms of correlation [11]. When 'm' numbers of variables in the data are dependent on other variables, the rank of the observed data set is less than the total number of variables (n). Correspondingly, the covariance matrix has 'm' zero valued Eigen values and the 'm' number of corresponding eigenvectors represent the linear relationships among the 'n' variables such that A. x=0, where the matrix A contains the transposed 'm' eigenvectors and x is the data without random noise. However, to represent the realistic situation, the relation Ay=r is considered instead of Ax=0, where r is supposed to be close to zero in no-fault situation and y= x+e is the noisy data vector which is the sum of the true data vector x and the white noise vector e. Since the rows of 'A' are transposed columns of the eigenvectors of the covariance matrix of (n×n) dimensional data matrix Y= $[y_1 y_2 \ldots . y_n]$, where$y_i \in R^n$, the first step in the PCA would be the eigenvalue-eigenvectordecomposition of the covariance matrix. The correlated variables are then projected onto the directions dictated by the eigenvectors to arrive at the uncorrelated latent variables. There the uncorrelation results in due to the orthogonality of the new axis or eigenvectors directed towards the variability's in the data. These eigenvectors of the data matrix are divided into two groups: the group which contains the large eigen values that explain the principal components subspace of the data and the group of small eigen values that span the residual subspace or null space. The latter group forms the matrix 'A', discussed above [10, 12]. In the following, the mathematical modeling of PCA is discussed in brief.

Let us take a data matrix X $\in R^{n\times m}$which consists of n rows and m columns can be normalized to zero mean and unit variance. Then matrix X can be decomposed into a score matrix T and a loading matrix P whose columns are the right singular vectors of matrix X are given by equation (1):

.

$$X = TP^T + \tilde{X} = TP^T + \tilde{T}\tilde{P}^t, \quad (1)$$

Where, $\tilde{X} = \tilde{T}\tilde{P}T$ is the residual matrix, if a scaled data sample is to be tested for a possible fault, it is decomposed as

$$X = \hat{X} + \tilde{X}, \quad (2)$$

where $\hat{X} = PP^T$, is projected on the principal component subspace and $\tilde{X} = (1 - PP^T)X$, is projected on the residual subspace if any change in sample X from the normal correlation takes place it can change the projections on to two subspaces whichthen

the magnitude of either $\tilde{X}$or $\hat{X}$ over the values obtained changes with normal data. The Square Prediction Error (SPE) measures the lack of fit of a model to the experimental data. The SPE statistic indicates the difference between its projections and samples in to k components retained in the model as

$$SPE=\|\bar{x}\|^2=\|(1-PP^T)\,x\|^2 \quad (3)$$

It is in normal condition when $SPE \leq \delta_\alpha{}^2$ (4)

Where $\delta_\alpha{}^2$ is a SPE's confidence limit.

$$\delta_\alpha{}^2 = \theta_1\left[\frac{C_\alpha\sqrt{2\theta_2}\square_0^2}{\theta_1}+1+\frac{\theta_2\square_0(\square_0-1)}{\theta_1^2}\right]^{1/\square_0} \quad (5)$$

Where, $\theta_i = \sum_{j=A+1}^{m}\lambda_j^i (i=1,2,3),$ (6)

$$\square_0 = 1-\frac{2\theta_1\theta_2}{3}, \quad (7)$$

λ_j is the Eigen value of covariance matrix X, $C_\alpha$is the threshold value within the confidence level α for the standard normal distribution, *m* is the number of principal components retained for residual subspace and*A* is the PCA model.

3.1. Wavelet Analysis

Transformations are general to apply when it is difficult to obtain the desired features from the original variables. If the original variables are time-domain signals, for some applications we also know about the frequency characteristics of a signal so for this Fourier transform analysis is used. This analysis discloses the variations in the frequency components in the signal. The drawback with Fourier transform is that it gives about the frequency components only but when this frequency is obtained at particular is not obtained. So this drawback is overcome by using, a wavelet function analysis. It can be applied to the signal to obtain three-dimensional information from the signals in the space to time frequency and amplitude. This is nothing but adding frequency information to a simple time-amplitude version, simply to know the occurrence of frequency components as a function of time [9].

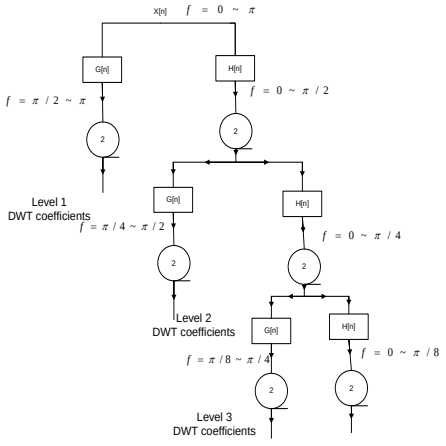

Fig. 1: Multi resolution analysis of wavelet transforms.

Discrete wavelet transform also called as the multi resolution analysis is depicted in **Figure 1**. The discrete wavelet transform is computed when a signal is passed through the series of low pass and high pass filters. After then sampling performed, which is of two types up sampling and down sampling. Up sampling increases the sampling rate and down sampling reduces it.

The **Figure 1** shows the 3-level DWT where H[n] and G[n] are the high pass and low pass filters. The scaling used is down sampling by a factor of 2. The signal has frequency component from 0 to π radians. For first level the signal is passes through series of high pass and low pass so the signal is divided into two parts 0 to $\pi/2$ and $\pi/2$ toπ. After that, down scaling of 2 is processed.

The frequency range of the signal at every level is marked on the **Figure 1** as "f".

The Wavelet Transform is computed by shifting, scaled version of wavelet function Ψ (t) and which is integrated and multiplied by the signal (t). The wavelet transformation C (a,b) for a signal s(t) is defined as in equation (8):

$$C(a,b) = \int_R s(t)\frac{1}{\sqrt{a}}\Psi\left(\frac{t-b}{a}\right)dt \quad (8)$$

$a \in R^+ - \{0\}$
$b \in R$

Where 'a' and 'b' are the discrete variables known as scaling parameter and time localization parameter respectively. And these are discrete variables. Each coefficient is multiplied by a particular scaled and shifted wavelet gives the certain part of the wavelet corresponding original signal. The signals with finite energy, the reconstruction formula for continuous wavelets are

$$s(t) = \frac{1}{K_\Psi}\int_R\int_{R+} c(a,b)\frac{1}{\sqrt{a}}\Psi\frac{t-b}{a}\frac{da}{a^2}db \quad (9)$$

$$K_\Psi = \int_{-\infty}^{+\infty}\frac{\Psi(\xi)^\wedge}{|\xi|}d\xi$$

The discrete wavelet analysis is described as

$C(a,b)=C(i,j)=\Sigma_{n\varepsilon Z}s(n)\Psi_{j,k}(n)$.

(4.3) (j,k) ∈ z^2: a = 2^j, b = 2^jk , Z= {0,±1,±2 .....} (j,k) ∈ z^2: $\Psi_{j,k}= 2^{-j/2}\,\Psi(2^{-j}t-K)$,

a = 2^j, b = 2^jk , j ∈ Z, k ∈ Z.

The inverse transform, also known as discrete synthesis is defined as

$$S(n)=\Sigma_{j\varepsilon Z}\Sigma_{k\varepsilon Z}C(j,k)\Psi_{j,k}(n). \quad (10)$$

The detail and approximation at level j are defined as

$$D_j(t)=\Sigma_{k\varepsilon Z}C(j,k)\Psi_{j,k}(t). \quad (11)$$

$A_{j-1} = \Sigma_{j>J}D_j$

And the following equations must agree

$A_{j-1} = A_j + D_j$, $s = A_j+\Sigma_{j-1}D_j$.

4. Multi-scale PCA

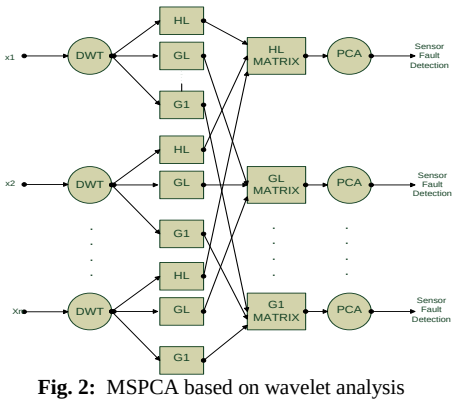

Fig. 2: MSPCA based on wavelet analysis

MSPCA is the technique used for FDI, basing on the two methods namely wavelet analysis and PCA. Here these two extract both the correlation within the sensors and cross correlation among the sensors. In MSPCA faults are detected using the SPE method and the diagnosis is done by the SPE contribution method. So here the contribution is a technique applied to each and every sensor present in the system to detect which sensor is most affected by fault [12-14].

In process monitoring MSPCA (**Figure 2**) first of all at each scale we have to compute independent principal components loadings for the scores and residuals for normal conditions detection limits violates. When a fault occurs then it represents a new data in which significant change is present. So when residuals present in the new data is computed from wavelet coefficients. The limits detected are violated for recent measurements at any scale. Since wavelet coefficients are the representation of high pass filters that means the sudden change occur the frequency component increases so it is detected by the details of the function. Here the change in frequency persist in feature at finest scale are detected first represented in abnormal condition. If this change is existed long time then these are indicated by corsair scales of the wavelet coefficients. For these wavelet coefficients the scaling functions at last approximation coefficients are detected as violate the limits in abnormal conditions after that it enters in to normal conditions. Likewise the process returns in to the normal operation values but the approximation coefficient represents the abnormal values due to corsair scale of representation. The combination with wavelets and PCA doesn't always give quick and continuous fault detection and also create false alarms. So, for this the last step is MSPCA to avoid the false alarms. This is done by reconstruct the signal in to time domain and for this signal compute the scores and residuals this improves the speed of fault detection at abnormal conditions.

5. Simulation model of the induction motor

The proposed simulation model of the three phase induction motor which has the rotor is short-circuited. The input mechanical torque is applied on the shaft i.e. 11.9 Nm as the full load torque. A three-phase motor rated 5.4 HP,400V, 1530 rpm, is fed by a sinusoidal PWM inverter is considered. The sinusoidal reference wave of base frequency is 50 Hz while the triangular carrier wave's frequency is set to 1980 Hz. The time step has been limited to 10 μs. This results into relatively high switching frequency (1980 Hz) of the inverter. Standard Simulink blocks are used to build the PWM inverter. The output of the PWM inverter goes through Controlled Voltage Source blocks. The motor has a set of 3 balanced currents for the phases *a*, *b* and *c* as shown in the **Figure 3**. It may be noted that though they are almost equal as a function of time, they are displaced by 120 electrical degrees from each other.

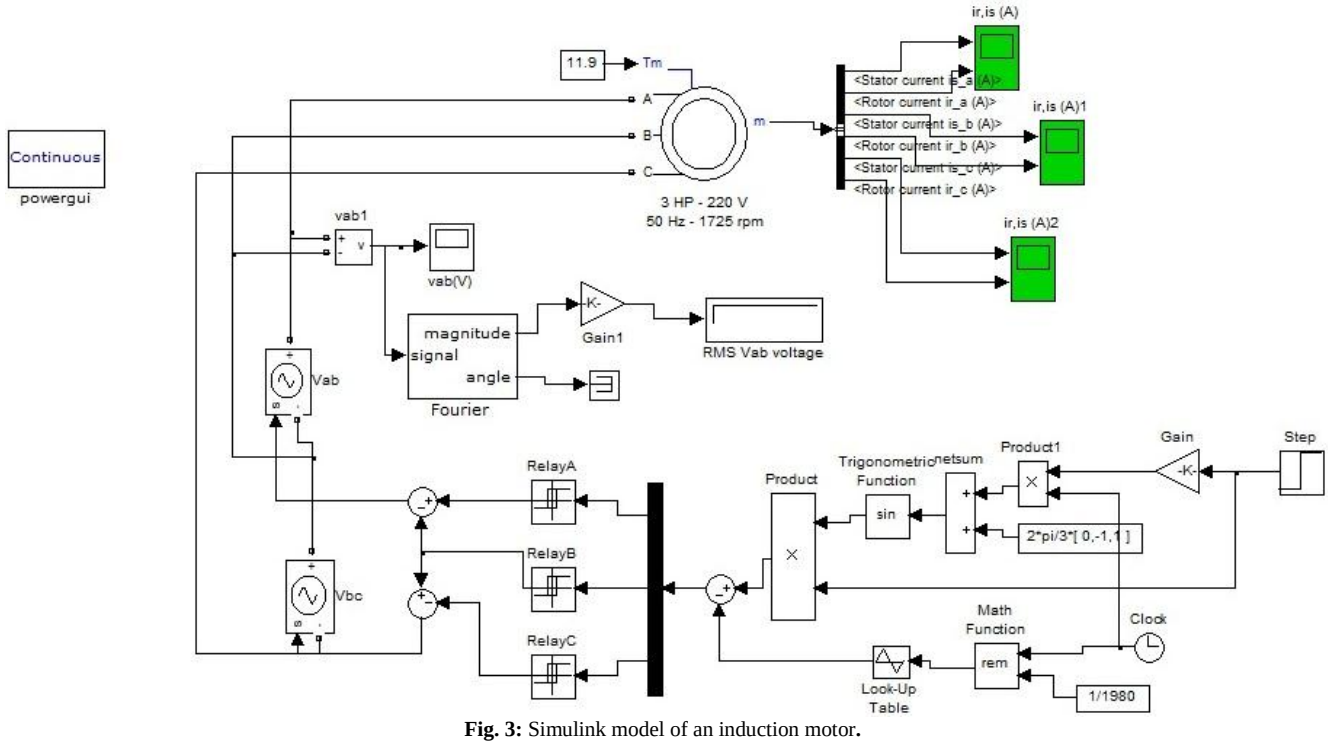

Fig. 3: Simulink model of an induction motor.

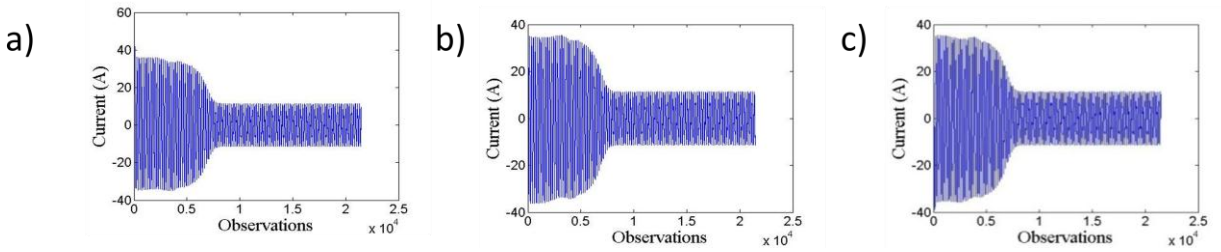

Fig. 4: Stator currents of the motor for (a) phase-a, (b) phase-b, and (c) phase-c

6. Results and Discussion

In this section, the results of MSPCA based FDI, when applied to the stator current data of induction motor, are presented. Though the data immediately after switching ON is obtained through simulation, only the portion with steady-state is considered for the

analysis. Different scenarios each concerned about a kind of fault or its changed magnitude are presented. It should be noted that though a single stator current is sufficient for the frequency based FDI, the analysis here considers all the three stator currents not only since the MSPCA based FDI requires at least three signals but also since the fault, if any, in one of the current sensors can be identified through PCA, whose model compares the signals for equality.

6.1. Case-1: No faults and noise-free data

The noise-free data in the case of no motor faults is considered as a special case. Three-level decomposition is considered for which the details and the approximation coefficients are as shown in **Figure 5**.

The FFT for this data is as shown in **Figure 6** from which it is evident that the frequency spectrum is around the fundamental frequency of 60 Hz. This indicates that there is no side-band frequencies representative of the faults mentioned in Section 2.

The FDI outcomes are as shown in **Figure 7**. There are no faults indicated by the MSPCA based FDI algorithm. This is expected as the data is corresponding healthy motor and there is no measurement noise from the current sensors.

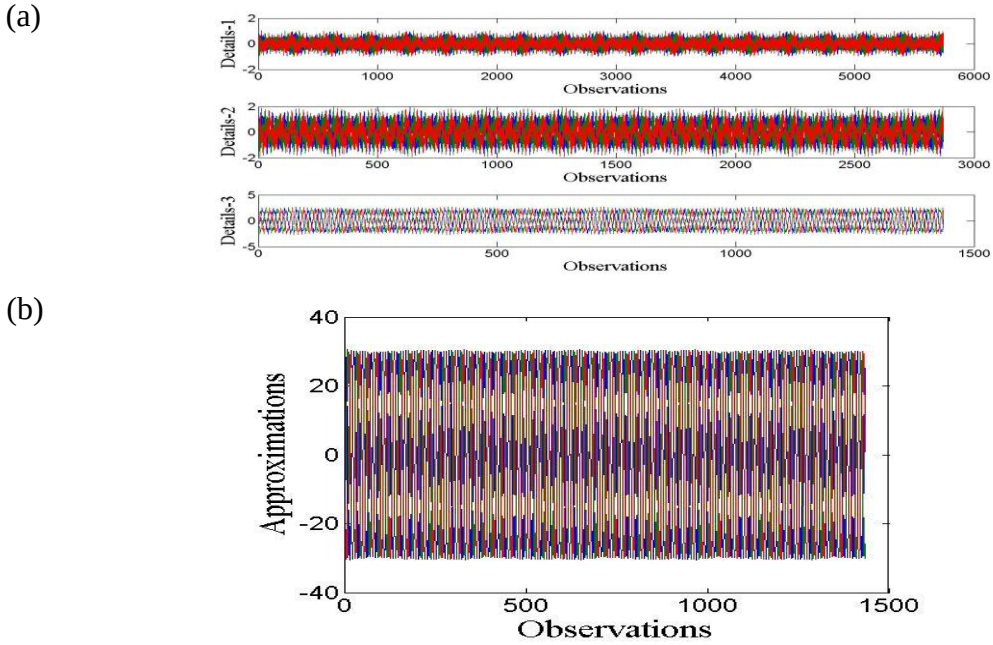

Fig. 5: The decomposition for case-1: (a) details; (b) approximations.

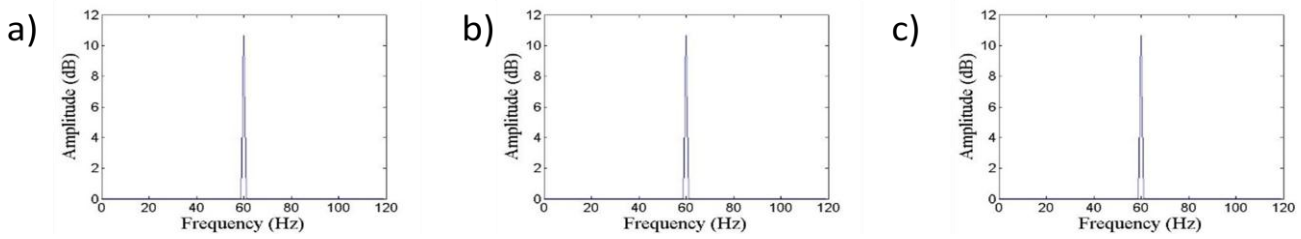

Fig. 6: The FFT plots for stator currents of (a) phase-a, (b) phase-b, and (c) phase-c.

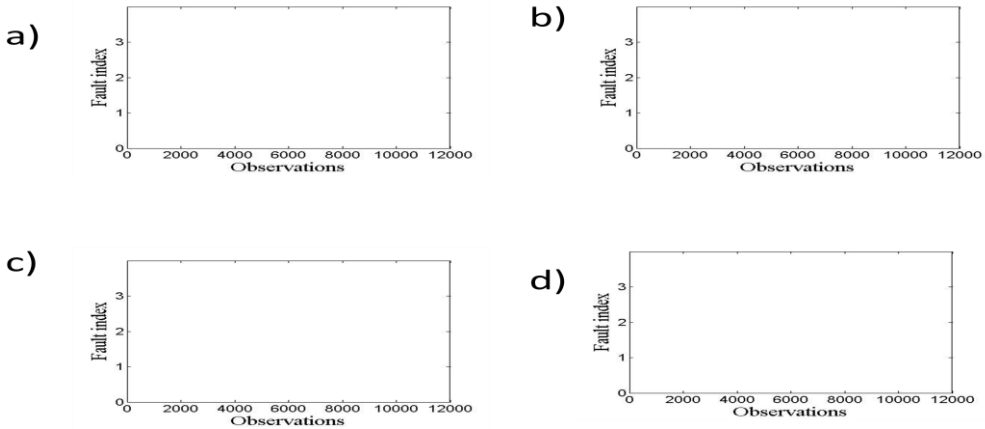

Fig. 7: FDI Outcomes for case-1: (a), (b) and (c) respectively with details 1, 2 and 3; (d) with approximations.

.2. Case-2: No-Faults but Noisy Data

In this case, a suitable noise is injected into the data of the current sensors to represent a realistic situation. The noise is considered to be normally distributed with mean value 0 and standard deviation of 0.1605. This value of standard deviation is 2% of the RMS value of the stator current, which is 8 A. The details, approximations, FFT plots of the stator currents and FDI outcomes are similar to that obtained for case-1. This is also expected from the scheme as the noise is to be tolerated and should not be considered as a fault. For brevity, the above characteristics are not shown here.

6.3. Case-3: Fault in the Machine and the Noisy Data

In this case, a fault in the machine with side-band frequencies 55 Hz and 65 Hz is considered. This is a representative situation for any one of the fault types mentioned in Section 2. The FFT plot of the currents in three phases is as shown in **Figure 8**. It should be noted that the plots for phases-b and c are quite similar, as the fault has equal impact on all the stator currents. It can be seen from **Figure 5,** the fault has similar effect on the phase currents, the index of the fault is shown equally among all phases with one of phases indicated as faulty at a time. The **Figure 9a-c** give the fault indices at different scales while **Figure 9d** represent the same at the low-frequency approximations. It can be said from the results that the fault has been successfully detected at all scales of the wavelet decomposition.

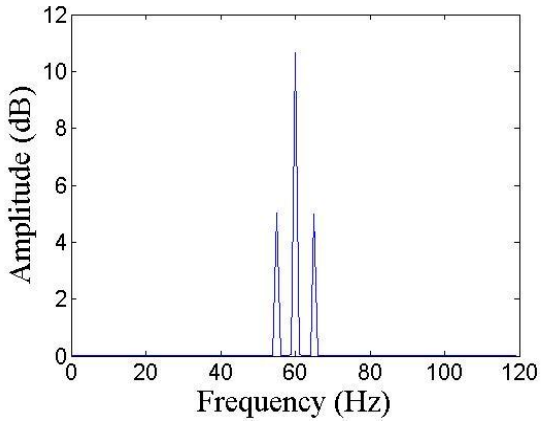

Fig. 8: The FFT plots in case-3 for stator currents of phase-a.

6.4. Case-4: Sensor Fault and Noisy Data

In this case, a current sensor fault has been considered while there is no fault in the motor. The algebraic relationships among the current sensor signals captured by PCA model makes the SPE violate the limit for healthy condition. When a constant bias of 5 A is added in the current sensor of phase-c (its value is more than others by 5 A), the difference is correctly identified as seen from the FDI indices of **Figure 10.** Hence, it can be said that the MSP-CA based algorithm has the capability of detecting the sensor faults along with the successful identification of the motor faults.

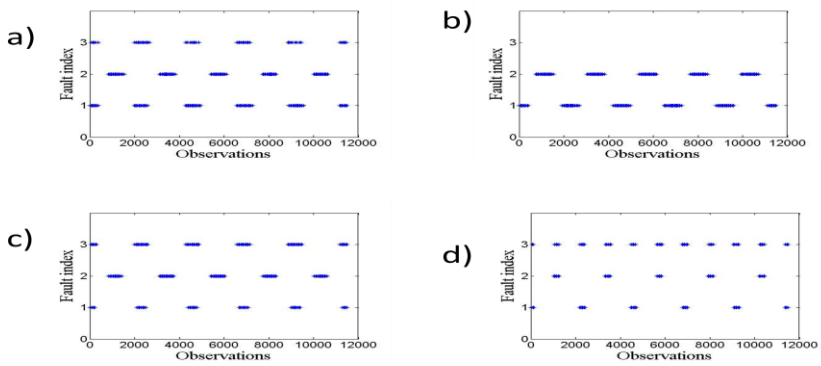

Fig.9: FDI Outcomes for case-3: (a), (b) and (c) respectively with details 1, 2 and 3; (d) with approximations

.

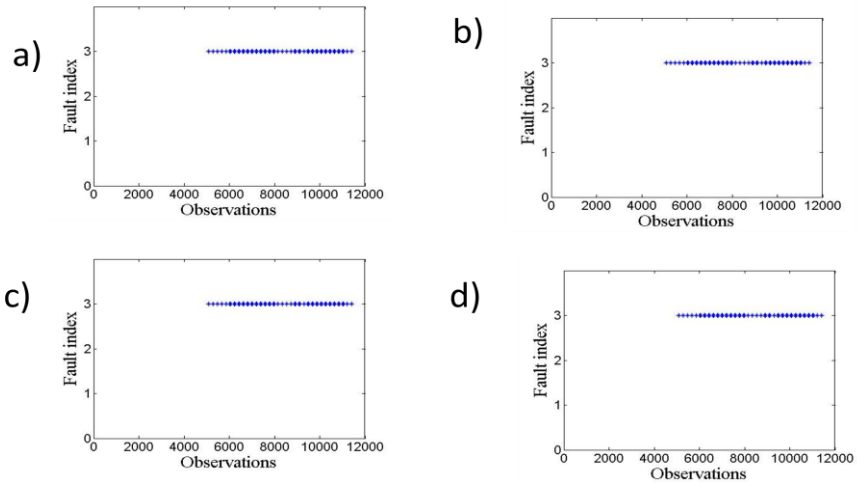

Fig.10: FDI Outcomes for case-4: (a), (b) and (c) respectively with details 1, 2 and 3; (d) with approximation.

7. Conclusions

Faults may occur during the operation of the induction motor. Some faults have the feature of producing some characteristic changes in the frequency of the stator currents. If these characteristic changes can be identified, diagnosis of the faults can be made. In this paper, the efficacy of the MSPCA based FDI has been reported, when applied to the data from the simulation model of an induction motor. Results indicated that the scheme has good capability to detect and identify the motor faults along with the sensor faults. However, tuning of the individual scales to identify one of the fault types is left for future scope.

References

[1] Cesarde coasta, Masamori kashiwgi, "Mauro hugomathias "Rotor failure detection of induction motor by wavelet transform and Fourier transform", *Case Studies in Mechanical Systems and Signal Processing* 1 (2015) 15–26.

[2] Mohamed E., Hachemi Benbowid., "A Review of Induction Motor Signature Analysis BE a Medium for Faults Detection", *IEEE Tram. Ind Eletronics.* 47, 5, (2000).

[3] H. Douglas, P. Pillay, A. K. Ziarani, "A New Algorithm for Transient MCSA Using Wavelets", *IEEE Transactions on Industry Applications*, 40, 5, (2004).

[4] Bashir Mahdiebrahimi, Novel indices for broken rotor bar fault diagnosis in induction motor using wavelet transform", *Mechanical systems and signal processing*., 30, (2012), 131-145.

[5] Yvon Tharrault, Gilles Mourot, José Ragot, Didier Maquin. "Fault detection and isolation with robust principal component analysis", *16th Mediterranean Conference onControl and Automation*, 18, 4, (2008), 429–442.

[6] Siti Nur Suhaila Mirin, Norhaliza Abdul Wahab, "fault detection and montoring using multi scale pca" *IEEE 4th Control and System Graduate Research Colloquium*, (2013), 19 – 20.

[7] Ye Zhongming. "A review on induction motor online fault diagnosis", *Proceedings IPEMC 2000 Third International Power Electronics and Motion Control Conference*, (2000).

[8] Partha Sarathee, Prakash Mangal, "Fault diagnostic and monitoring methods of induction motor: a review," *International Journal of Applied Control, Electrical and Electronics Engineering*, (2013) 1-18.

[9] Malik Abadulrazzaq Alsaedi, "Fault Diagnosis of Three-Phase Induction Motor: A Review, *Optics" Special Issue: Applied Optics and Signal Processing*.4, 1-1, (2015), 1-8. doi: 10.11648/j.optics.s.2015040101.11

[10] Jackson, J.E. "a user's guide to principal components" *Wiley-Interscience, New York*, (2003)

[11] Misra M., "Multivariate process monitoring and fault diagnosis by multi-scale PCA", *Computers and Chemical Engineering*, (2002), 0915

[12] Jackson, J., Mudholkar "Control procedures for residuals associated with principal component analysis". , *Technometrics*, 21, 341–349.

[13] Manish M., Yuea H. H., Qin S. J., Ling B., "multivariate process monitoring and fault diagnosis by multi-scale pca", *Computers & Chemical Engineering*, 26, (2002), 1281–1293.

[14] Wang, Zhanfeng, Hailian Du, Feng Lv, and Wenxia Du. "The fault detection of multisensor based on multi-scale PCA" , *25th Chinese Control and Decision Conference (CCDC)*, (2013).